

Scattering polarization of hydrogen lines in the presence of turbulent electric fields

R. Casini and R. Manso Sainz[‡]

High Altitude Observatory, National Center for Atmospheric Research[§]
P.O. Box 3000, Boulder, CO 80307-3000, U.S.A.

E-mail: casini@ucar.edu, rsainz@iac.es

Abstract.

We study the broadband polarization of hydrogen lines produced by scattering of radiation, in the presence of isotropic electric fields. In this paper, we focus on two distinct problems: a) the possibility of detecting the presence of turbulent electric fields by polarimetric methods, and b) the influence of such fields on the polarization due to a macroscopic, deterministic magnetic field. We found that isotropic electric fields decrease the degree of linear polarization in the scattered radiation, with respect to the zero-field case. On the other hand, a distribution of isotropic electric fields superimposed onto a deterministic magnetic field can generate a significant increase of the degree of magnetic-induced, net circular polarization. This phenomenon has important implications for the diagnostics of magnetic fields in plasmas using hydrogen lines, because of the ubiquitous presence of the Holtsmark, microscopic electric field from neighbouring ions. In particular, previous solar magnetographic studies of the Balmer lines of hydrogen may need to be revised because they neglected the effect of turbulent electric fields on the polarization signals. In this work, we give explicit results for the Lyman α and Balmer α lines.

PACS numbers: 32.60.+i, 32.80.Bx, 52.25.Os

[‡] Now at the Instituto de Astrofísica de Canarias, Vía Láctea s/n, E-38200 La Laguna, Tenerife, Spain

[§] The National Center for Atmospheric Research is sponsored by the National Science Foundation

Table 1. Holtsmark normal field strengths of microturbulent electric fields in hydrogen plasmas of laboratory and astrophysical interest.

Object	N (cm ⁻³)	E (V cm ⁻¹)	E (e.s.u.)
Interstellar gas	1	$3.75 \cdot 10^{-7}$	$1.25 \cdot 10^{-9}$
Gaseous nebula	10^3	$3.75 \cdot 10^{-5}$	$1.25 \cdot 10^{-7}$
Solar Corona	10^9	$3.75 \cdot 10^{-1}$	$1.25 \cdot 10^{-3}$
Solar Corona, solar transition region	10^{10}	1.74	$5.80 \cdot 10^{-3}$
Solar Chromosphere, solar prominences	10^{11}	8.08	$2.69 \cdot 10^{-2}$
Solar T minimum, diffuse hot plasma	10^{12}	$3.75 \cdot 10^1$	$1.25 \cdot 10^{-1}$
Solar Photosphere, gas discharge	10^{14}	$8.08 \cdot 10^2$	2.69
Thermonuclear plasma	10^{15}	$3.75 \cdot 10^3$	$1.25 \cdot 10^1$
Dense hot plasma	10^{18}	$3.75 \cdot 10^5$	$1.25 \cdot 10^3$
Laser plasma	10^{20}	$8.08 \cdot 10^6$	$2.69 \cdot 10^4$

1. Introduction

Radiation scattering by a plasma is due to the processes of photon absorption and re-emission by the atoms in the plasma. During absorption, atomic polarization (i.e., population imbalances and quantum coherences between atomic sublevels) can be created, depending on the angular distribution and polarization of the incident radiation (*optical pumping*).

In the presence of external fields, the natural degeneracy of the angular-momentum sublevels is removed, so these sublevels evolve at slightly different frequencies. As a consequence, the atomic polarization—and therefore the polarization of the re-emitted radiation—is modified in a way that depends on the strength and orientation of the external field (e.g., by the Hanle effect). It is noteworthy that the scattering polarization does not necessarily cancel out even if the external fields are isotropically distributed, unless the atomic excitation processes (either radiative or collisional) are also isotropic. The phenomenon of (partial) depolarization of the scattered radiation due to isotropically distributed magnetic fields has been extensively investigated [1, 2, 3, 4]. In the case of hydrogen, because of its sensitivity to electric fields to first order of perturbation (*linear Stark effect*), we must expect that the line polarization due to radiation scattering be significantly affected by both magnetic and electric fields.

This suggests two interesting problems, which are related. The first problem concerns the possibility of detecting turbulent electrostatic fields by polarimetric methods. The fields can be either microscopic (due to neighboring ions) or macroscopic (due to plasma turbulence) [5]. The second problem concerns the effect of turbulent electric fields on the polarization signals generated in the presence of a deterministic magnetic field, and the consequences for the diagnostics of macroscopic magnetic fields using hydrogen lines.

Table 1 lists approximate values for the strength, E , of a microscopic electric field acting on an atom as a function of the perturbing ion density, N , in the plasma. These

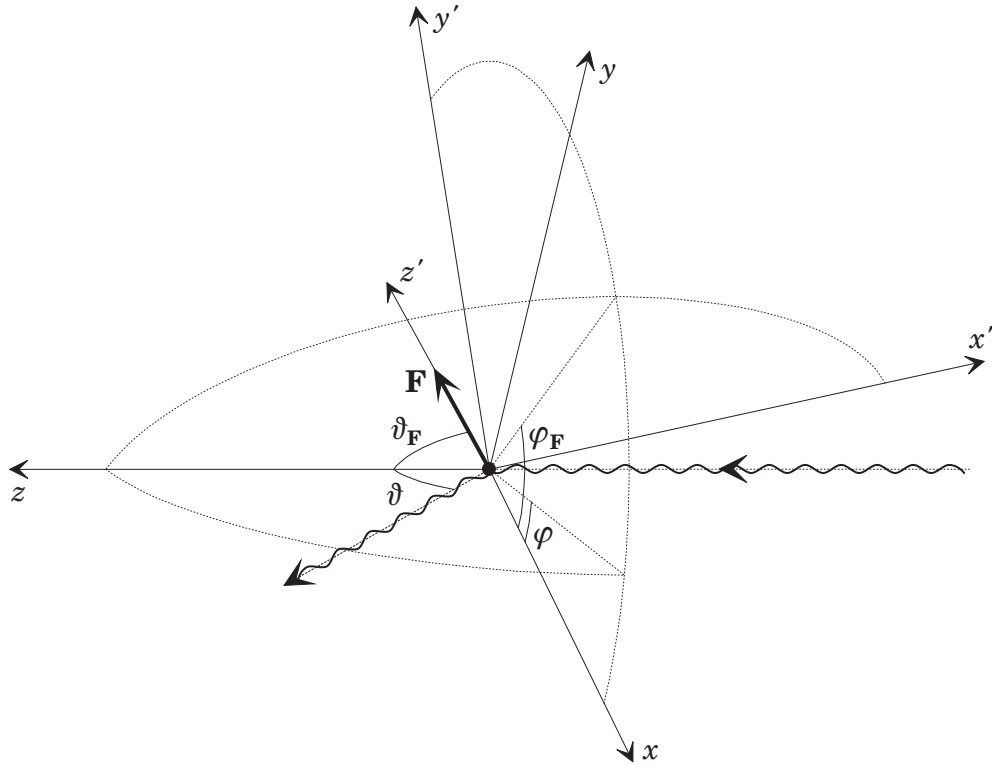


Figure 1. General geometry for the description of the scattering of radiation in the presence of an external field. The pair $(\vartheta_{\mathbf{F}}, \varphi_{\mathbf{F}})$ specifies the direction of the external field, \mathbf{F} , in the reference frame $S \equiv xyz$, whereas the pair (ϑ, φ) specifies the direction of the scattered radiation. The reference frame $S' \equiv x'y'z'$ is the one adopted for the solution of the statistical equilibrium of the atomic system subject to the external field and to the incident radiation along z , and it is obtained from the original frame S by means of a rotation of $\varphi_{\mathbf{F}}$ around z plus a rotation of $\vartheta_{\mathbf{F}}$ around y' .

values are calculated as the Holtmark normal field strength characteristic of a random distribution of neighboring ions [5]. They illustrate the limit of the electric contribution to scattering polarization that must be expected under different plasma conditions.

In Section 2, we will study the scattering polarization of hydrogen lines in the presence of isotropically distributed magnetic or electric fields. In Section 3, we investigate instead the case in which the scattering polarization due to a deterministic magnetic field of various orientations is modified by the additional presence of an isotropic distribution of electric fields. In this work we only present results for the Lyman α ($\text{Ly}\alpha$) and Balmer α ($\text{H}\alpha$) lines, although we verified the generality of our conclusions for all hydrogen transitions up to level $n = 4$.

2. Scattering polarization in the presence of randomly oriented fields

The general expression for the emissivity in the four Stokes parameters [6, 4], I , Q , U , and V , for a gas of hydrogen atoms subject to electric and magnetic fields, was given in [7], assuming L - S coupling. Here we consider broadband (i.e., frequency-integrated)

polarization signals, in which case the line emissivity for a transition from an upper level of principal quantum number n_u to a lower level n_ℓ , in a gas of atomic density N , is [7]

$$\begin{aligned} \varepsilon_i(\mathbf{k}) = & \frac{e_0^2 a_0^2}{\sqrt{3} \pi c^3} N \omega_{n_u n_\ell}^4 \sum_{L_u L'_u L_\ell} \sum_{J_u J'_u} \sum_{KQ} (-1)^{L_u + L'_u + L_\ell + S + J'_u + K + 1} \\ & \times \Lambda(n_u L_u, n_\ell L_\ell) \Lambda(n_u L'_u, n_\ell L_\ell) \sqrt{(2J_u + 1)(2J'_u + 1)} \\ & \times \begin{Bmatrix} L_u & L'_u & K \\ 1 & 1 & L_\ell \end{Bmatrix} \begin{Bmatrix} L_u & L'_u & K \\ J'_u & J_u & S \end{Bmatrix} T_Q^K(i, \mathbf{k})^{n_u S} \rho_Q^K(L_u J_u, L'_u J'_u), \end{aligned} \quad (1)$$

where $i = 0, 1, 2, 3$ enumerates the four Stokes parameters. In eq. (1), $\omega_{n_u n_\ell}$ is the Bohr frequency of the transition, and

$$\Lambda(nL, n'L') = \sqrt{(2L + 1)(2L' + 1)} \langle nL | r | n'L' \rangle \begin{pmatrix} L & L' & 1 \\ 0 & 0 & 0 \end{pmatrix},$$

where the dipole-matrix element is calculated using Gordon's formula [8]. The angular distribution of the emitted radiation is determined by the irreducible spherical tensors $T_Q^K(i, \mathbf{k})$ ($K = 0, 1, 2$, and $Q = -K, \dots, K$), where \mathbf{k} is the propagation direction. The explicit expressions of these tensors are tabulated, for example, by [9, 4, 7]. Figure 1 illustrates the relevant geometric quantities for the description of radiation scattering in the presence of an external field.

For a given illumination, the irreducible spherical components of the density matrix, ${}^{nS} \rho_Q^K(L_u J_u, L'_u J'_u)$, are calculated in the limit of statistical equilibrium, taking into account the relaxation and transfer of atomic polarization between levels, because of absorption and emission processes, as well as the level mixing induced by the external fields [7]. In particular, the self-consistent treatment of level mixing within our formalism allows us to consider all possible regimes of magnetic and electric fields in a unified way, including the magnetic and electric Hanle effects, the linear Zeeman and Stark effects in both the strong- and weak-field limit (i.e., both "normal" and "anomalous" effects), as well as the incomplete Paschen-Back effect for both magnetic and electric fields (which characterizes the actual regimes for level crossing). It is important to notice that magnetic fields only mix atomic sublevels with the same L , whereas electric fields only mix sublevels with $\Delta L = \pm 1$. For arbitrary field geometries, both fields mix sublevels with different J 's and M 's. Thus, in the presence of both electric and magnetic fields, only the principal quantum number, n , remains a good quantum number. || We will consider an atomic model of hydrogen including the Bohr levels $n = 1, 2, 3, 4$. Therefore, the excitation state of the atomic system is described by $4 + 64 + 324 + 1024 = 1416$ density matrix elements ${}^{nS} \rho_Q^K(L_u J_u, L'_u J'_u)$. These form the solution of a 1416×1416 linear system, which must be solved numerically. In this solution, all allowed radiative transitions within the atomic model are considered simultaneously and consistently. So the contributions of both elastic (Rayleigh) and inelastic (Raman) scattering to the broadband polarization of the scattered radiation are properly taken into account.

|| We limit our investigation to field strengths for which configuration mixing between different n levels can be neglected.

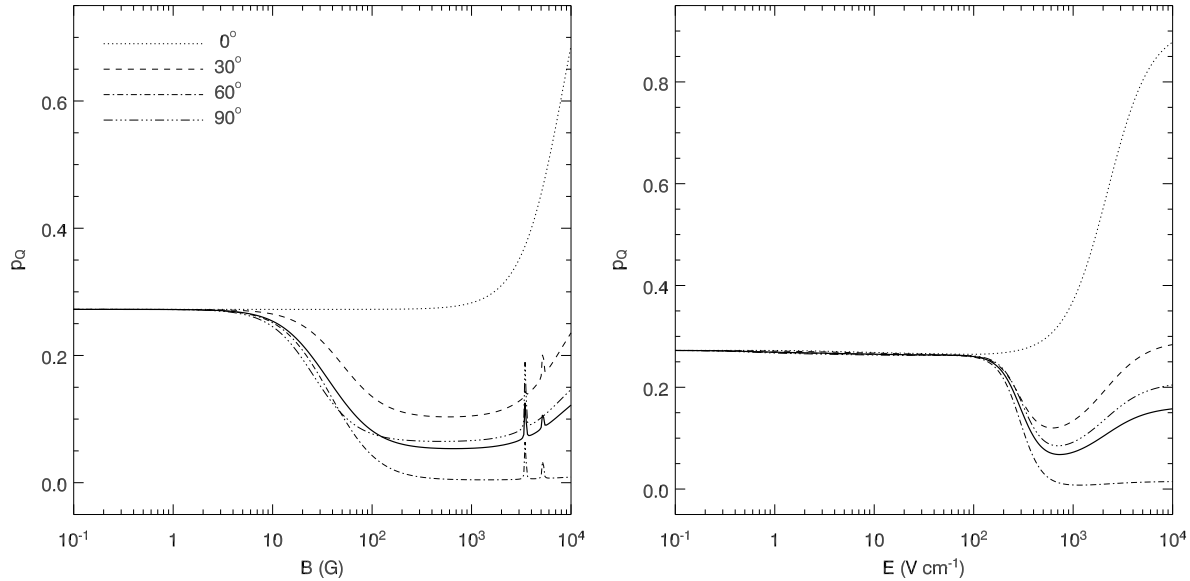


Figure 2. Broadband, fractional linear polarization of the Ly α line of hydrogen in a 90 $^\circ$ -scattering event, as a function of the strength of a randomly oriented magnetic field (left panel) and electric field (right panel). The thick solid line corresponds to the case of isotropic fields, while the discontinuous lines show the contributions of azimuth-averaged fields of various inclinations $\vartheta_{\mathbf{F}}$. Because of the symmetry properties of the scattering process, the curves for $\vartheta_{\mathbf{F}}$ and $180^\circ - \vartheta_{\mathbf{F}}$ are identical.

To investigate the effects of isotropically distributed fields, we must calculate the average $\langle \varepsilon_i(\mathbf{k}) \rangle_{(\vartheta_{\mathbf{F}}, \varphi_{\mathbf{F}})}$ over all possible field orientations $(\vartheta_{\mathbf{F}}, \varphi_{\mathbf{F}})$ within the sphere. In practice, we compute $\varepsilon_i(\mathbf{k})$ for a finite number of directions, $(\vartheta_{\mathbf{F}}^i, \varphi_{\mathbf{F}}^j)$, determined as the nodes of some angular quadrature over the sphere, and then we sum the results with the appropriate weights $w_{i,j}$ given by the quadrature formula.

For the case considered in this section, it is possible to perform the analytic integration over the field azimuth, $\varphi_{\mathbf{F}}$, for any given value of the field inclination, $\vartheta_{\mathbf{F}}$, because of the axial symmetry of the problem around the propagation direction of the incident radiation. In order to see this, we consider in detail the form of eq. (1). The geometric tensors, $T_Q^K(i, \mathbf{k})$, are expressed in the reference frame that has the field direction as its polar axis (which we indicate with z' ; see Fig. 1). They are obtained from the same tensors in the reference frame specified by the incident radiation via the transformation [10]

$$T_Q^K(i, \mathbf{k}) = \sum_{Q'} D_{Q'Q}^K(R_{zz'}) T_{Q'}^K(i, \mathbf{k})_z, \quad (2)$$

where $R_{zz'}$ is the rotation operator that carries the z -frame into the z' -frame. The rotation matrix in eq. (2) is

$$D_{Q'Q}^K(R_{zz'}) = \exp(-iQ'\varphi_{\mathbf{F}}) d_{Q'Q}^K(\vartheta_{\mathbf{F}}), \quad (3)$$

since the third Euler angle of the transformation can arbitrarily be set equal to zero in this case. The azimuth of the scattering direction in the z -frame, φ , enters the expression

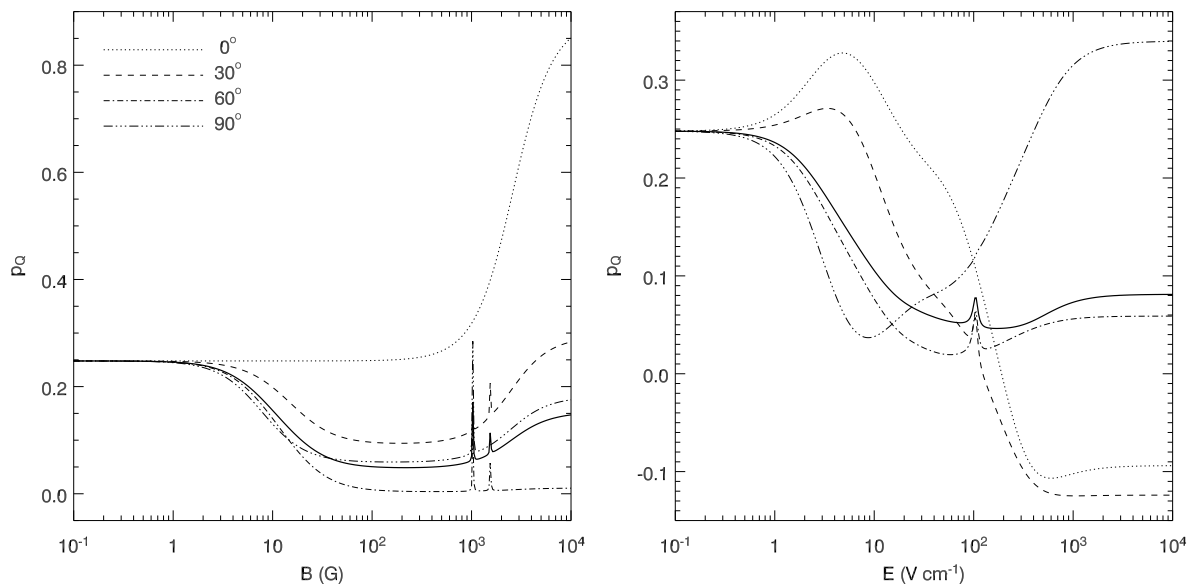


Figure 3. Same as Fig. 2, but for the H α line of hydrogen.

of the geometric tensors $T_Q^K(i, \mathbf{k})_z$ in such a way that it is possible to factor it out, since (see Table I in [7])

$$T_Q^K(i, \mathbf{k})_z = t_Q^K(i, \mathbf{k}) \exp(iQ\varphi), \quad (4)$$

where the tensors $t_Q^K(i, \mathbf{k})$ no longer depend on φ . The azimuthal average of $T_Q^K(i, \mathbf{k})$ is then (cfr. eq. [2])

$$\begin{aligned} \langle T_Q^K(i, \mathbf{k}) \rangle_\varphi &= \sum_{Q'} d_{Q'Q}^K(\vartheta_{\mathbf{F}}) t_{Q'}^K(i, \mathbf{k}) \langle \exp[iQ'(\varphi - \varphi_{\mathbf{F}})] \rangle_\varphi = d_{0Q}^K(\vartheta_{\mathbf{F}}) t_0^K(i, \mathbf{k}) \\ &\equiv d_{0Q}^K(\vartheta_{\mathbf{F}}) T_0^K(i, \mathbf{k})_z. \end{aligned} \quad (5)$$

From a physical point of view, averaging eq. (1) over the azimuth of the scattering direction for a given magnetic field must be equivalent to averaging instead over the azimuth of the magnetic field for a fixed scattering direction. Therefore, using the averages (5) in eq. (1), in place of the original tensors $T_Q^K(i, \mathbf{k})$, is equivalent to computing the scattered radiation from an elemental volume of plasma embedded in a field of random azimuth $\varphi_{\mathbf{F}}$.

Figures 2 and 3 show the broadband, fractional linear polarization, p_Q , of the Ly α and H α lines of hydrogen (at 121.5 nm and 656.3 nm, respectively) in a 90 $^\circ$ -scattering event, as a function of the field strength of randomly oriented magnetic and electric fields. (Because of the symmetry of the problem, $p_U \equiv 0$, and therefore p_Q contains the entire information of linear polarization.) In those figures, we show the case of fields that are isotropically distributed in azimuth for various inclinations $\vartheta_{\mathbf{F}}$ from the z -axis (discontinuous lines), and the case of fields that are instead completely isotropic within the unit sphere (continuous thick line). The case of completely isotropic fields is calculated using an 8-point Gaussian quadrature of the solutions for random-azimuth fields at appropriate inclinations [11]. Because of the symmetry properties of the Hanle

effect in 90° scattering, it is possible to consider only the hemisphere with $\vartheta_{\mathbf{F}} \leq 90^\circ$, since the polarization curves for $\vartheta_{\mathbf{F}}$ and for $180^\circ - \vartheta_{\mathbf{F}}$ are identical. For the calculations of these plots, we assume that the atom is illuminated by a collimated beam of radiation corresponding to a Planckian intensity at 20 000 K.

We see that random-azimuth fields can produce either an increase or a decrease of the broadband linear polarization with respect to the field-free scattering polarization, depending on the field strength, and also on the field inclination with respect to the direction of incident radiation. However, the overall trend for isotropically distributed fields within the sphere is always one of depolarization of the scattered radiation.

The strong resonances shown in the left panels of Figs. 2 and 3 correspond to different crossings between magnetic sublevels within the upper levels of the transitions. In a ^2P term, the two sublevels $M = +1/2$ and $M = -1/2$ of the $^2\text{P}_{1/2}$ level cross the sublevel $M = -3/2$ of the $^2\text{P}_{3/2}$ levels respectively at $\omega_B = (4/9)\omega_{\text{FS}}$ and $\omega_B = (2/3)\omega_{\text{FS}}$, where ω_B is the Larmor frequency for the applied field, and ω_{FS} is the fine-structure separation between the two J levels of the term [4, 8]. In the particular case of hydrogen, these crossings occur at $B = 3483$ G and $B = 5225$ G in the 2^2P term, and at $B = 1032$ G and $B = 1548$ G in 3^2P term. Because at level crossing the atomic system tends to recover the polarization state that characterizes the absence of Hanle depolarization (corresponding to the curves for vertical magnetic fields in Figs. 2 and 3), these level-crossing resonances produce important peaks in the scattering polarization signal [12, 13]. Because in a 90° -scattering event only the $\Delta M = \pm 2$ crossings contribute to scattering polarization when $\vartheta_{\mathbf{B}} = 90^\circ$, the resonance for $\omega_B = (2/3)\omega_{\text{FS}}$ disappears from our plots for such inclination of the field [12].

The resonance of the $\text{H}\alpha$ polarization for $E = 104.5$ Vcm $^{-1}$, visible in the right panel of Fig. 3, has an analogous physical explanation. It corresponds to the crossing between pairs of sublevels with $|M| = 1/2$ and $|M| = 3/2$ that are attributable to the $3^2\text{P}_{3/2}$ term in the limit of vanishing fields.

It must be noted that the effects of level crossing take place in an interval of Larmor frequencies (magnetic or electric) comparable in width to the inverse of the lifetime of the levels involved. Thus the width of the associated resonances must also be comparable to that of the interval within which the Hanle-effect depolarization (seen as a gentle slope immediately following the initial plateau in Figs. 2 and 3) takes place. Since the level-crossing resonances occur at much larger Larmor frequencies (comparable to the fine-structure separation) than the Hanle depolarization, they appear as very sharp peaks in our figures, because of the logarithmic scale adopted for the field strength.

The depolarization of hydrogen line radiation in the presence of isotropic electric fields has important consequences for the diagnostics of magnetic fields in laboratory and astrophysical plasmas. For example, it is customary in solar plasma diagnostics to assume that depolarization of the scattered radiation is indicative of the magnetic Hanle effect (and possibly, of collisional depolarization), and therefore it is used to infer the magnetic field in the plasma. The fact that an isotropic distribution of electric fields as low as 10 V cm $^{-1}$ (i.e., a Holtmark field typical of the plasma density of the solar

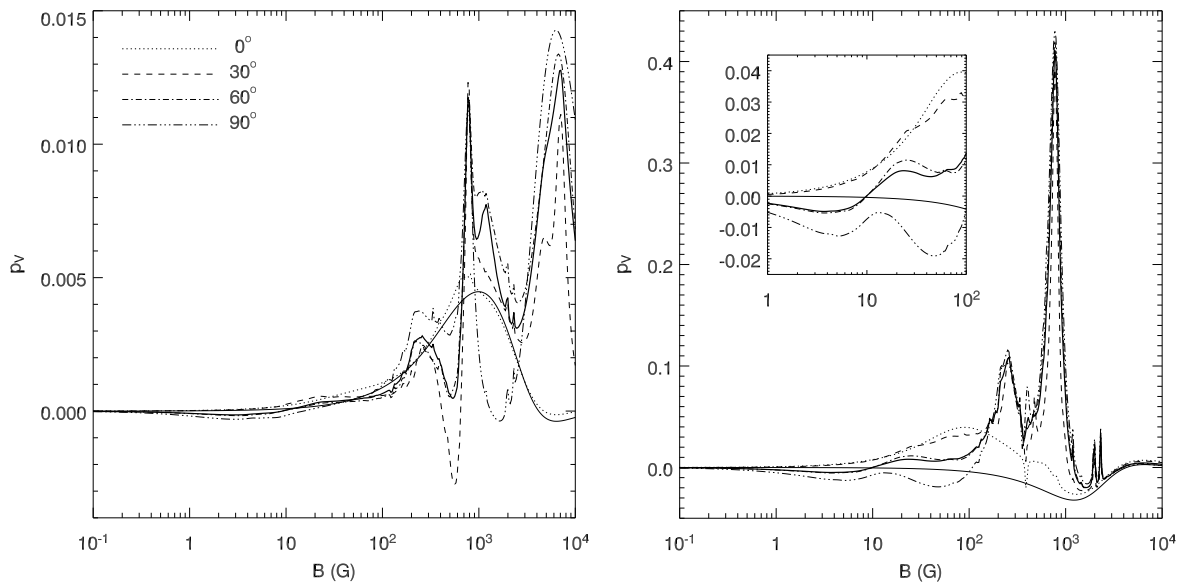


Figure 4. Broadband, fractional circular polarization of the Ly α (left panel) and H α (right panel) radiation in a forward scattering event, as a function of the strength of a magnetic field directed along the line-of-sight, and in the additional presence of a randomly oriented electric field with $E = 10 \text{ V cm}^{-1}$. The thin solid line corresponds to the solution without electric fields. The thick solid line corresponds to the case of isotropic electric fields, while the discontinuous lines show the contributions of azimuth-averaged electric fields of various inclinations $\vartheta_{\mathbf{E}}$. Because of the symmetry properties of the scattering process, the curves for $\vartheta_{\mathbf{E}}$ and $180^\circ - \vartheta_{\mathbf{E}}$ are identical. The insert in the right panel shows an enlargement of the plot of the net circular polarization of H α for vertical magnetic fields between 1 G and 10^2 G.

atmosphere; see Table 1) can be largely responsible for the depolarization of the scattered radiation of the H α line of hydrogen is a result that must be taken into consideration for any modeling of the magnetic Hanle effect of this commonly observed line.

3. Scattering polarization in the presence of a deterministic magnetic field and a microturbulent electric field

In this section we study the scattering polarization of hydrogen lines in the simultaneous presence of a deterministic magnetic field and a microturbulent electric field.

We first examine the case of forward scattering with the magnetic field directed along the line-of-sight (i.e., the z -axis of Fig. 1). In this geometry, the symmetry considerations of the previous section still hold, because the magnetic field preserves the cylindrical symmetry of the illumination process. So we can calculate the scattering polarization for a random-azimuth distribution of electric fields by averaging over the azimuth of the line-of-sight for a fixed azimuth of the electric field, using eq. (5). Once again, the case of completely isotropic fields is calculated using an 8-point Gaussian quadrature of the solutions for random-azimuth fields at appropriate inclinations [11].

The presence of a magnetic field introduces a chirality in the system, which

is evidenced by the generation of a non-vanishing amount of broadband circular polarization (see Fig. 4, thin solid line). Ultimately this is determined by the presence of atomic orientation in the hydrogen levels, which is generated by the alignment-to-orientation (A-O) conversion mechanism [14, 15].

The additional presence of an isotropic electric field, as small as 10 V cm^{-1} , has a dramatic effect on the net circular polarization (NCP), as illustrated by Fig. 4 (thick solid line). That figure also shows the contributions of electric fields with different inclinations with respect to the magnetic field. Electric fields parallel to the magnetic field alter quantitatively the amount of NCP. However, electric fields not aligned with the macroscopic magnetic field make, in general, a qualitatively more diverse contribution to the NCP. This is due to the very complex pattern of level crossings and anti-crossings that is produced for crossed fields. In particular, we notice the remarkable resonance of the NCP of $\text{H}\alpha$ at $B \approx 800 \text{ G}$.

The reason why these structures are typically very broad (even in a logarithmic scale) is that the A-O mechanism takes place for a range of Larmor frequencies comparable to the fine-structure separation within an atomic term. In fact, the origin of the A-O mechanism is the interference between different J levels rather than level crossing itself. (However, when a level crossing occurs in the regime of the A-O mechanism, a sharp resonance of the NCP can be produced on top of the main structure.) The additional presence of an electric field, inclined with respect to the magnetic field, produces a sub-fine structuring of the atomic term (in the form of level anti-crossings), which modulate the NCP with additional structures of diverse width and amplitude.

The important effects of microturbulent electric fields on the NCP of $\text{H}\alpha$ must be taken into account when interpreting broadband filter observations of the circular polarization in this line. In fact, all too often the assumption is made that the longitudinal Zeeman effect, with its characteristic antisymmetric signature, is the only mechanism responsible for the observed signal. Then, a non-zero NCP is explained in terms of velocity gradients along the line-of-sight, or even as instrumental cross-talk that needs to be removed, thus missing out on an important physical aspect of hydrogen plasma spectroscopy.

Next we consider the case of a deterministic magnetic field oriented at 90° from the incident direction (horizontal field). We examine three fundamental scattering configurations for this case: a) forward scattering; b) 90° scattering with the magnetic field directed along the line-of-sight; and c) 90° scattering with the magnetic field oriented at 90° from the line-of-sight. Because the magnetic field no longer preserves the cylindrical symmetry of the scattering event, this time $\langle \varepsilon_i(\mathbf{k}) \rangle_{(\vartheta_{\mathbf{E}}, \varphi_{\mathbf{E}})}$ must be calculated using a numerical angular quadrature over the whole sphere. For this purpose, we adopted the 26-point quadrature given in [11].

Figure 5 shows the broadband, fractional linear polarization, $p_L = \sqrt{p_Q^2 + p_U^2}$, of the $\text{H}\alpha$ line of hydrogen for four different intensities (0, 1, 10, and 10^2 V cm^{-1}) of the microturbulent electric field. The magnetic regime below 10^2 G is dominated by

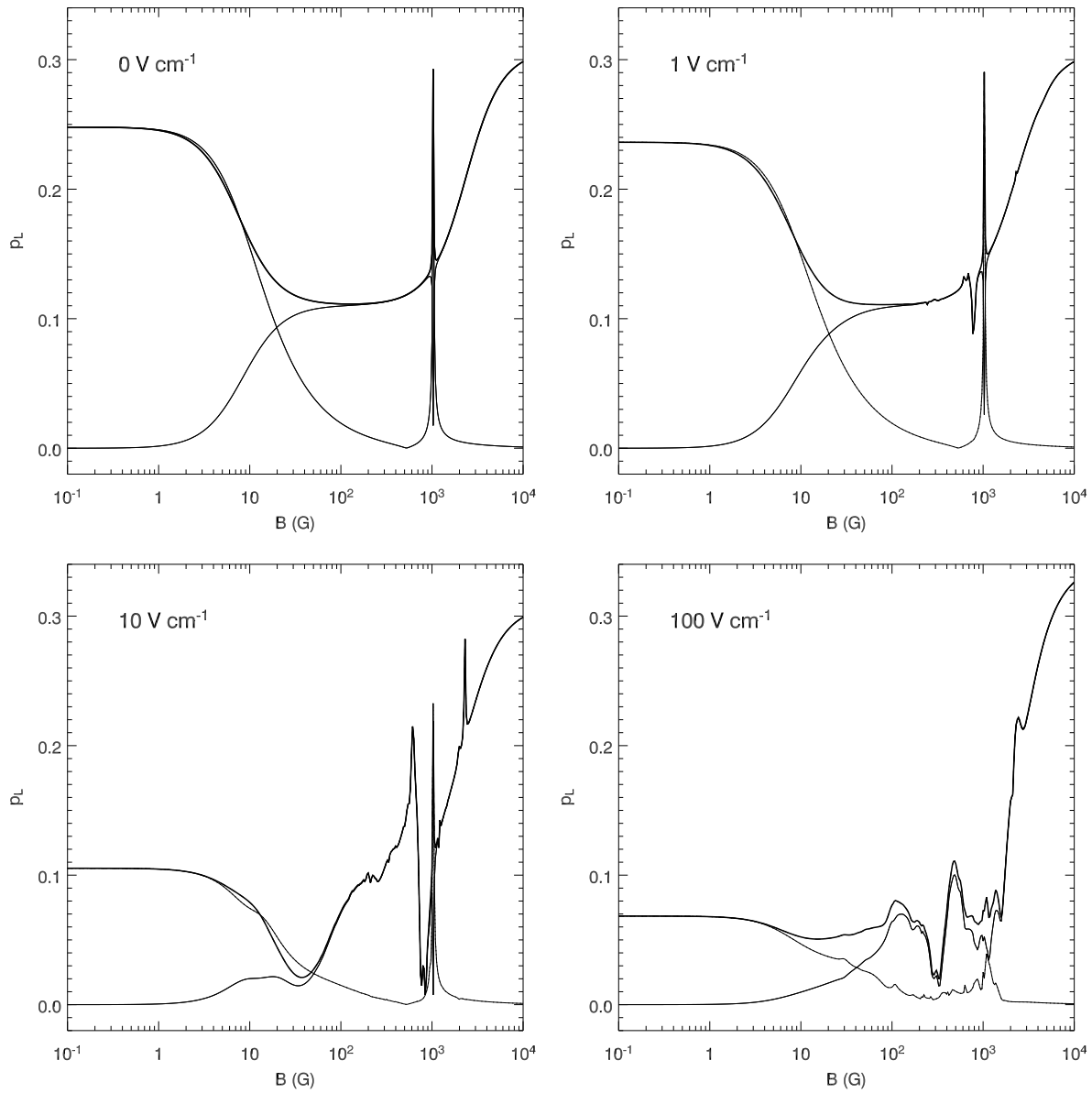


Figure 5. Broadband, fractional linear polarization of the $H\alpha$ line of hydrogen in the presence of a horizontal magnetic field, and for increasing strengths of a superimposed, isotropic electric field. The thin line corresponds to the case of forward scattering. The medium line corresponds to the case of 90° scattering, with the magnetic field directed towards the observer. Finally, the thick line corresponds to the case of 90° scattering, with the magnetic field at 90° from the line-of-sight. We notice that the “saturation” level for strong magnetic fields, transverse to the line-of-sight, is not constant for increasing electric strengths, as a result of the competing regimes for the normal Zeeman effect and the normal Stark effect.

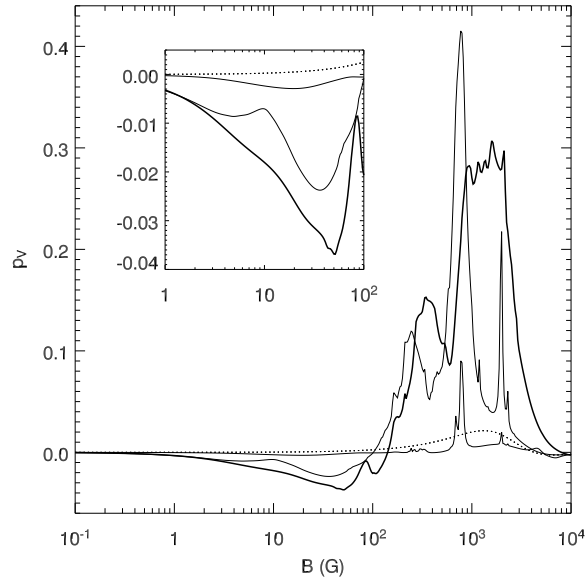


Figure 6. Net circular polarization of the $H\alpha$ line of hydrogen in a 90° scattering event, with a horizontal magnetic field directed towards the observer. Thin, medium, and thick solid lines correspond to the cases in which an isotropic electric field of 1, 10, and 10^2 V cm^{-1} , respectively, is also present. The dotted line represents the limit case with zero electric field. The insert shows an enlargement of the plot of the NCP of $H\alpha$ for horizontal magnetic fields between 1 G and 10^2 G.

scattering polarization, and its signal is an attenuated version of the limit case without electric fields (compare the panels of Fig. 5 for non-zero electric fields, with the right panel of Fig. 3). Instead, isotropic fields as weak as 10 V cm^{-1} significantly affect the linear polarization signal above 10^2 G.

The strong resonance at $B \approx 10^3$ G that is visible for $E \leq 10$ V cm^{-1} has already been discussed in the previous section, and it occurs for $\omega_B = (4/9)\omega_{\text{FS}}$, even in the absence of electric fields. In the particular field geometry adopted for these figures, the other resonance at $\omega_B = (2/3)\omega_{\text{FS}}$ is not visible. The addition of a microturbulent electric field as small as 10 V cm^{-1} modifies the energy structure of the hydrogen atom dramatically. As a consequence, the pattern of resonances in the $H\alpha$ polarization is also affected. In particular, we notice the negative resonance appearing around $B \approx 800$ G, which becomes more important with the increasing electric strength. This resonance has the same origin of the dominant peak in the right panel of Fig. 4, and it is due to an electric induced anti-crossing between the 3^2P and 3^2D terms. The sub-fine structure separation determined by anti-crossing levels increases with the electric strength, eventually lifting the level crossing at $\omega_B = (4/9)\omega_{\text{FS}}$. In the plots of Fig. 5, this phenomenon is illustrated by the increasing width of the resonance at $B \approx 800$ G, and the leveling out of the peak at $B \approx 10^3$ G for increasing electric strengths. Other resonances are also visible in those figures, appearing and disappearing as the energy structure of the atom is modified by the increasing electric field.

It is also interesting to consider the NCP for this new magnetic configuration.

Figure 6 illustrates the case of the $H\alpha$ line. The dotted line corresponds to the purely magnetic limit, showing the NCP generated by the A-O mechanism, mostly between 10^2 G and 10^4 G. It is notable the modification that microturbulent electric fields as weak as 1 V cm^{-1} already produce (thin solid line). In particular, we notice once again the resonance at $B \approx 800$ G. The effects determined by fields of 10 and 10^2 V cm^{-1} (medium and thick solid lines, respectively) are significantly larger, as expected.

In concluding this discussion, it is important to remark that such microturbulent fields are characteristic of ionic densities between 10^{11} and 10^{13} cm^{-3} , which are common in many astrophysical plasmas, like stellar atmospheres (see Table 1). In particular, the inserts in the right panel of Fig. 4, and in Fig. 6, show in details the modification of magnetic-induced circular polarization in the presence of microturbulent electric fields, for the restricted magnetic range $1 \text{ G} \leq B \leq 10^2 \text{ G}$. This is the regime of magnetic fields that can be expected in solar prominences, according to recent spectropolarimetric observations in the D_3 line of He I at 587.6 nm [16] (which, to first order, is insensitive to electric fields). On the other hand, according to our current knowledge of the electron density in these structures ($10^{10} \lesssim N_e \lesssim 10^{12} \text{ cm}^{-3}$ [17]), the average Holtmark field that can be expected is of the order of 10 V cm^{-1} (see Table 1). We see that for typical fields in solar prominences (the average field of quiescent prominences is around 20 G [16]), the presence of a microturbulent field characteristic of the electron density in those structures can induce a significant enhancement of the NCP of the $H\alpha$ line, which can easily exceed one order of magnitude, depending on the magnetic field strength and orientation. This result could explain recent observations of anomalous NCP of $H\alpha$ in solar prominences [18], which cannot be explained simply by invoking the A-O mechanism in the presence of magnetic fields alone.

It is important to understand in more detail the physical mechanism by which turbulent (as well as deterministic) electric fields are capable to induce a large degree of atomic orientation, when in the presence of a magnetic field, and why this can happen for significantly smaller magnetic strengths than in the case of the magnetic-induced A-O mechanism. As noted above, such mechanism of *electric re-orientation* is responsible for the appearance of a significant amount of NCP in the $H\alpha$ line, for magnetic strengths that are sufficiently small for the Zeeman-effect signal to be completely dominated by the intensity-like contribution of the atomic orientation. In [7], it was pointed out that this phenomenon can be traced back to the different pattern of level crossings and anti-crossings that is determined by the simultaneous presence of magnetic and electric fields. Here we want to make this argument more precise. The basic fact is that the A-O mechanism is efficient for Larmor frequencies of the order of the fine-structure separation between interfering levels. Because of the relatively large size of the fine structure in the lowest levels of hydrogen, this condition requires magnetic strengths in excess of 10^3 G. When an electric field is also present (whether deterministic or turbulent), quantum interferences can arise between different LS terms belonging to the same Bohr level. For example, the two levels $^2P_{3/2}$ and $^2D_{3/2}$ in the upper level of $H\alpha$ interfere with each other in the presence of an electric field, and their separation (Lamb shift) is about two

orders of magnitude smaller than the fine-structure separation within each term. For this reason, the A-O mechanism becomes already efficient for magnetic fields of the order of 10 G. For those magnetic strengths, the polarization amplitude of the Zeeman effect is very small, and so the circular-polarization profile is dominated by the contribution of the atomic orientation [7].

4. Conclusions

In this paper, we conducted a numerical study of the effect of turbulent electric fields on the scattering polarization of hydrogen lines. We first considered the case of a non-magnetic plasma, and successively the case in which a deterministic magnetic field is also present. We presented results for the Ly α and H α lines, which are the most relevant for laboratory and astrophysical plasma studies. However, our general conclusions apply as well to all other transitions within the model atom used for this work (Ly α , Ly β , Ly γ , H α , H β , Paschen α).

For the case of a non-magnetic plasma, we find that turbulent electric fields decrease the broadband linear polarization produced by scattering, analogously to the depolarization of the scattered radiation produced by turbulent magnetic fields through the magnetic Hanle effect [1, 2, 3, 4]. This electric depolarization must always occur in a hydrogen plasma, because of the ubiquitous, microscopically turbulent, electric fields produced by charged ions (mainly protons) surrounding the scatterer (Holtmark field; see [5] and Table 1). However, it must be expected also in the presence of macroscopically turbulent electric fields, as far as the spatial scale of plasma turbulence is much smaller than the photon mean free path in the plasma. For the case of a Holtmark field, the electric depolarization provides an independent polarimetric tool for plasma density diagnostics.

For the case of a magnetized plasma, we find that the magnetic scattering polarization is significantly modified by the additional presence of electric fields, even when these are isotropically distributed. In particular, we must expect a general decrease of the broadband, linear polarization by scattering in hydrogen lines that form in the presence of weak magnetic fields ($B \lesssim 10^2$ G; see Fig. 5). Obviously, this additional depolarization induced by turbulent electric fields must be taken into account in the magnetic Hanle-effect diagnostics of hydrogen lines formed in the presence of either deterministic or turbulent magnetic fields.

We also find that turbulent electric fields can be responsible for a significant enhancement of the NCP of hydrogen lines, for particular magnetic field strengths. For example, the many-fold enhancement of the NCP of H α (see Fig. 4 and 6), for gas densities typical of the solar chromosphere ($N_e \sim 10^{11}$ cm $^{-3}$; see Table 1), and for magnetic field strengths approximately between 1 and 10^2 G, provides a very simple explanation of recent measurements of anomalous levels of NCP in H α observed in solar prominences [18].

The results presented in this paper are of diagnostic interest for polarization studies

of magnetic plasmas in a large interval of electron densities. In particular, they also apply to quasi-equilibrium plasmas for which the magneto-hydrodynamic hypothesis excludes the possibility that deterministic electric fields can form in the reference frame of the magnetic sources. Therefore, the general conclusion of this investigation is that the effect of turbulent electric fields of statistical origin cannot be ignored in any polarimetric diagnostics of hydrogen lines in magnetized plasmas, because of the significant modification of the broadband polarization that these electric fields can produce. In particular, magnetogram techniques based on the observation of the $H\alpha$ line on the Sun should be carefully revised.

There are three principal limitations to our work. First of all, the line formation theory adopted for this work does not include collisions. It is possible that collisional depolarization might significantly affect our results by decreasing the amount of broadband polarization that can actually be achieved for a particular field geometry and illumination condition. In particular, this might reconcile our investigation with some polarimetric observations of $H\alpha$ that show only negligible amounts of broadband polarization.

A second limitation is that our results are obtained assuming an average strength for the turbulent electric fields (typically, the normal field strength of the Holtmark theory), rather than a more physically appropriate distribution of field strengths. However, the results of Section 2 can be generalized directly by convolving the curves in the right panels of Figs. 2 and 3 with the appropriate distribution of electric strengths. The same can be done for the case of turbulent magnetic fields (left panels of Figs. 2 and 3), given the distribution of magnetic strengths in the plasma. For the problems studied in Section 3, instead, one must necessarily engage in the more computationally intensive process of calculating the weighted average (following the electric strength distribution) of many realizations of the plots of Figs. 4–6.

The third simplifying hypothesis of our work, which should be investigated further, is the very assumption that the turbulent electric fields be isotropic. This seems a reasonable hypothesis in the absence of other deterministic fields (whether magnetic or electric), like the cases considered in Section 2. However, the additional presence of a deterministic field introduces a privileged direction, in response of which, for example, the ions in the plasma could organize themselves into anisotropic particle distributions, which ultimately would be responsible for anisotropic distributions of the perturbing electric fields [19, 20]. It would be very interesting to extend the methods illustrated in this paper to explore the possibility of detecting the spectro-polarimetric signature of such anisotropic distributions of ions in a plasma.

It must also be observed that the simple thermal agitation of the scattering atoms in a hot, magnetized plasma is directly responsible for the appearance of microturbulent electric fields of the $\mathbf{v} \times \mathbf{B}$ type, in the atomic rest frame. These, so-called *motional*, electric fields add an anisotropic term (lying on the plane normal to \mathbf{B}) to the microturbulent fields due to the charged perturbers, even when the latter can be considered to be isotropically distributed in the plasma. In particular, this opens the

intriguing possibility of a polarimetry-based diagnostics of plasma temperature.

It is evident that a quantitative analysis of real observations of the scattering polarization in magnetized hydrogen plasmas must take into account all possible causes of anisotropy of the distribution of the microturbulent electric fields—like the ones discussed above—for a correct diagnostics of the magnetic field.

References

- [1] Stenflo J O 1982 *Solar Phys.* **80** 209
- [2] Landi Degl’Innocenti M and Landi Degl’Innocenti E 1988 *Astron. Astrophys.* **192** 374
- [3] Stenflo J O 1994 *Solar Polarization* (Dordrecht: Kluwer Academic)
- [4] Landi Degl’Innocenti E and Landolfi M 2004 *Polarization in Spectral Lines* (Dordrecht: Kluwer Academic)
- [5] Griem H R 1974 *Spectral Line Broadening by Plasmas* (New York: Academic Press)
- [6] Born M and Wolf E 1983 *Principles of Optics (6th ed.)* (Oxford: Pergamon Press)
- [7] Casini R 2005 *Phys. Rev. A* **71** 062505
- [8] Bethe H A and Salpeter E E 1957 *Quantum Mechanics of One- and Two-Electron Atoms* (New York: Academic Press)
- [9] Bommier V *Astron. Astrophys.* **328** 726
- [10] Brink D M and Satchler G R 1993 *Angular Momentum* (Oxford: Clarendon Press)
- [11] Abramowitz M and Stegun I A 1964 *Handbook of Mathematical Functions* (Washington: National Bureau of Standards)
- [12] Bommier V 1980 *Astron. Astrophys.* **87** 109
- [13] Moruzzi G and Strumia F 1990 *The Hanle Effect and Level-Crossing Spectroscopy* (New York: Plenum Press)
- [14] Lehmann J C 1969 *Phys. Rev.* **178** 153
- [15] Kemp J C, Macek J H and Nehring F W 1984 *Astrophys. J.* **278** 863
- [16] Casini R, López Ariste A, Tomczyk S and Lites B W 2003 *Astrophys. J.* **598** L67
- [17] Tandberg-Hanssen E 1995 *The Nature of Solar Prominences* (Dordrecht: Kluwer Academic)
- [18] López Ariste A, Casini R, Paletou F, Tomczyk S, Lites B W, Semel M, Landi Degl’Innocenti E, Trujillo Bueno J, and Balasubramaniam K S 2005 *Astrophys. J.* **621** 145L
- [19] Sholin G V and Oks E A 1973 *Dokl. Akad. Nauk. SSSR* **209** 1318 [1973 *Sov. Phys. Dokl.* **18** 254]
- [20] Deutsch C and Bekefi G 1976 *Phys. Rev. A* **14** 854